

The GISS Global Climate-Middle Atmosphere Model. Part II: Model Variability Due to Interactions between Planetary Waves, the Mean Circulation and Gravity Wave Drag

D. RIND, R. SUOZZO,* AND N. K. BALACHANDRAN**

Goddard Space Flight Center, Institute for Space Studies, New York, N.Y.

(Manuscript received 3 April 1987, in final form 20 April 1987)

ABSTRACT

The variability which arises in the GISS Global Climate-Middle Atmosphere Model on two time scales is reviewed: interannual standard deviations, derived from the five-year control run, and intraseasonal variability as exemplified by stratospheric warmings. The model's extratropical variability for both mean fields and eddy statistics appears reasonable when compared with observations, while the tropical wind variability near the stratopause may be excessive, possibly due to inertial oscillations. Both wave 1 and wave 2 warmings develop, with connections to tropospheric forcing. Variability on both time scales results from a complex set of interactions among planetary waves, the mean circulation, and gravity wave drag. Specific examples of these interactions are presented, which imply that variability in gravity wave forcing and drag may be an important component of the variability of the middle atmosphere.

1. Introduction

Climate changes driven by the increase of trace gases with greenhouse properties may alter the physical and chemical composition of the middle atmosphere (approximately 10–100 km). This possibility can be evaluated through the use of appropriate general circulation models, in a manner similar to that employed for investigations of future tropospheric changes (e.g., Schlesinger and Mitchell, 1987). The GISS Global Climate/Middle Atmosphere Model (GCMAM), an extension of the global tropospheric climate model to include the middle atmosphere, has been developed for this purpose. The paper describing the model's climatology (Rind et al., 1988, henceforth Part I) emphasized its ability to produce reasonable simulations of the time-averaged fields. To ensure that these results have not been achieved through the use of parameterizations which rigidly tune the model to observed climatology, it is necessary to compare the model's natural variability with that of the observational data. This will not ensure that the model has the appropriate sensitivity to changes induced by climate perturbations, but it will help evaluate the model's inherent flexibility.

The middle atmosphere real world variability exists

on a variety of time scales. There is substantial interannual variability, especially during the development of the winter stratosphere and the final spring warming. Variability occurs within a month, associated with events such as stratospheric warmings. Variability on both of these time scales results from changes in the dynamical forcing by the troposphere, or in the ability of this forcing to propagate into the stratosphere (e.g., Hamilton, 1982; Davies, 1981). The ability of the model to simulate such effects is an important indication of the realism of its dynamical interactions, and both time scales will be explored below. Variability also occurs associated with the diurnal cycle, and is indicative of the model's ability to directly generate thermally driven long gravity waves (tides). The model-generated diurnal and semidiurnal tides will be discussed in a separate publication.

Both interannual and intraseasonal variability in the model result from interactions among planetary waves, the mean circulation, and the parameterized gravity wave drag. Since the model gravity wave influence is quantifiable, the complex interactions can be diagnosed in a manner as yet unavailable for the real atmosphere. To the extent that the model realistically portrays the atmospheric dynamical developments, it can provide some insight into the operative processes and feedbacks. Thus, in the evaluation of model variability, we focus on the types of interactions which appear to be occurring among the three features.

2. Model interannual variability

Results presented below are from the model 2 version of the GCMAM discussed in Part I, which was run for five years following a spin-up of ten months

* Sigma Data Service Corporation, New York, N.Y. 10025.

** Lamont-Doherty Geological Observatory of Columbia University, Palisades, New York 10964.

Corresponding author address: Dr. David Rind, Goddard Space Flight Center, Institute for Space Studies, 2880 Broadway (Room 636), New York, NY 10023.

done with model 1. As noted in Part I, the first two years were run with the Coriolis force set to zero at the pole, as in the standard UCLA model code (Arakawa, 1972), while the last three years used the full value for this term, as in the nine-layer GISS model 2 (Hansen et al., 1983). Since the difference between these formulations affects the circulation only near the pole, the standard deviations will be shown from the full five-year run except for the values at the latitude closest to the pole in each hemisphere, which will generally be for the last three years.

Model and observed monthly standard deviations for the zonal mean wind and wave 1 amplitude during December–February are shown in Fig. 1. The model zonal wind variability in the extratropics is in excellent agreement with observations; we show below reasons for the variability in the model.

In the tropics, the model variability is associated with an apparent inertial instability (which also occurred in model 1), and which may be exacerbated by the gravity wave drag from the moist convective source. The establishment of a band of winds in the longitude–height wind profile causes waves of a given phase speed to break in the vicinity of this band, which then causes the waves to tend to accelerate the band toward the wave phase speed. Previous runs with stronger moist-convective drag resulted in more pronounced bands; however, the banded profile itself arose in model 1 (without gravity wave drag) when inertial instability criteria were met, as described in Part I. The instability is relatively symmetric, occurring at all longitudes, at altitudes below 50 km, but is characterized by substantial longitudinal asymmetry in the mesosphere; the reason for this variation with altitude is not yet understood. The effect is to produce oscillations in the equatorial wind profile, so that while a five-year monthly average shows a semiannual oscillation (Part I, Fig. 3), the wind at a particular altitude may be quite different from one year to the next. Hitchman and Leovy (1986) report large shears and possible inertial instability near the stratopause in wind fields derived from LIMS data.

The monthly standard deviations of the contributions to the zonal wind forcing are shown in Fig. 2. Note that the standard deviations of the eddy forcing (EP flux divergence), transformed mean circulation effect, and gravity wave drag are all of the same order of magnitude, indicating that all three are contributing significantly to the modeled interannual variability. The standard deviations of the zonal wind changes due to the transformed advection and the gravity wave drag both amount to 10%–25% of their average monthly value (Part I, Figs. 4–7) and they are very similar to one another. This is due at least in part to the generation of a portion of the transformed streamfunction by the gravity wave drag. The standard deviation of the eddy forcing represents up to 100% of its monthly mean

value, the result of eddy-produced events such as the two stratospheric warmings discussed below.

Standard deviations of the hemispheric energy budgets and conversions have been shown in Part I, Table 4. The model's Northern Hemisphere zonal kinetic energy interannual variability for winter ranges from 18% of the mean in the lower stratosphere, to 28% of the mean in the mesosphere. The largest contributing factors to this variability arise due to changes in sign of energy cycle conversions and dissipation processes (Part I, Table 4), again emphasizing the role of planetary wave and gravity wave effects.

The variability of standing wave 1 is shown in Fig. 1. Overall the model and observed variabilities are very similar, but in the lower stratosphere, model variability is somewhat too small. The modeled long-wave amplitudes are also generally smaller than the observed in this region (Part I, Table 3). The Northern Hemisphere winter eddy kinetic energy standard deviation in the model peaks at 17% of the mean in the upper stratosphere, with values of about 7% in the lower stratosphere and mesosphere (Part I, Table 4). The variability is only 4% in the troposphere, emphasizing that for the hemisphere as a whole, small changes in tropospheric energy are all that is necessary to produce significant alterations in the middle atmosphere structure.

The gravity-wave momentum flux impinging on the stratosphere, generated by the parameterization which is a function of model-resolved processes in the troposphere, has relatively large standard deviations during December–February, on the order of the monthly mean value (Fig. 3; compare with the average source magnitudes, given in Part I, Figs. 8, 9). Thus, part of the variability observed in the model stratosphere arises from tropospheric variability of both planetary waves and gravity waves. In agreement with the results indicated in Figs. 2 and 3, we show that at least in the model, variability in tropospheric gravity wave sources needs to be considered in discussions of stratospheric changes.

The model variability of wind and temperature at three different pressure levels is shown in Fig. 4. In the lower stratosphere, both parameters are extremely repeatable from year to year, in agreement with observations (e.g., Oort and Peixoto, 1983). In the middle stratosphere, variability peaks in the winter hemispheres, with maxima occurring in the Northern Hemisphere during December–January (when warmings develop) and during March. This latter effect is due to the variability in timing of the final spring warming in the model, which is affected by the dynamic history of the winter (e.g., Finger and Teweles, 1964). Large wind variability also occurs in the tropics, as discussed above. At higher levels, maximum wind variability occurs near the summer pole, a region in which the easterlies are being affected by gravity-wave

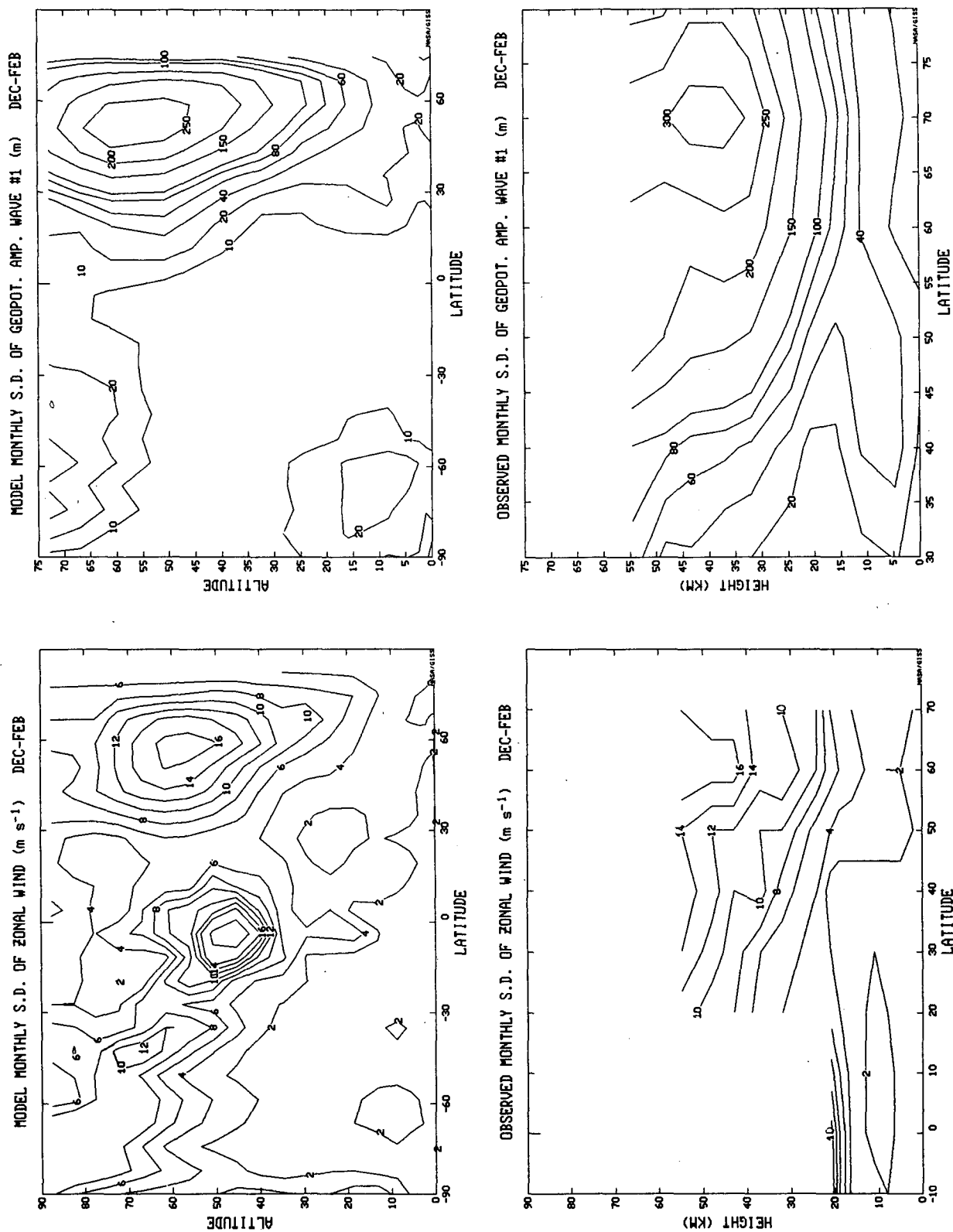


FIG. 1. Monthly average standard deviations of the zonal mean wind (left) and for the geopotential amplitude of wavenumber 1 (right) from the model (top) and observed (bottom) for Dec-Feb. The standard deviations were calculated for each month separately and then averaged. Model standard deviations for the zonal wind grid box nearest the pole are from the last three years (with the full value of the Coriolis parameter); at all other locations, from the five years. The observed zonal wind standard deviations for the troposphere are from Oort (1977), while at higher levels they are calculated from seven years of observations shown by Quiroz (1981) and Geller et al. (1984). The observed standard deviation of wavenumber 1 amplitude is calculated from the four years of data shown by Geller et al. (1984).

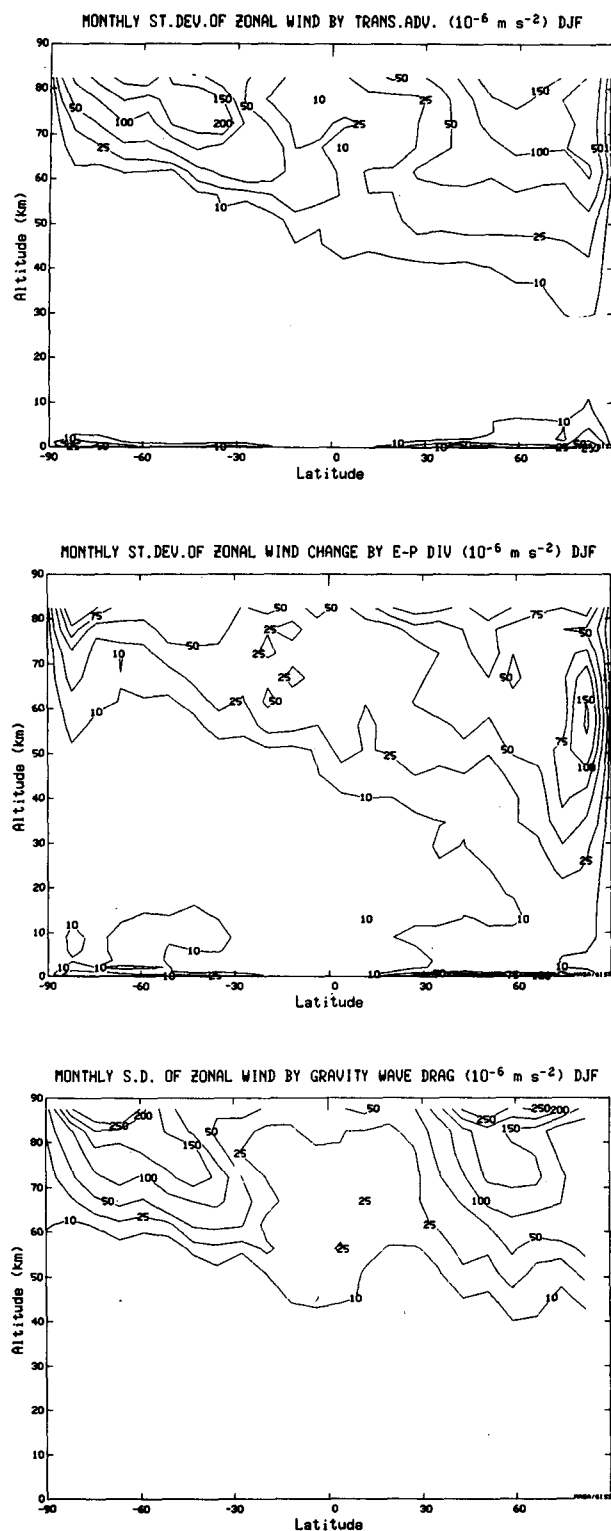


FIG. 2. Monthly average standard deviations of the terms contributing to changes in the zonal mean wind, averaged over the months of December to February. Shown are the standard deviations of the zonal wind change due to transformed advection (top), due to the EP flux divergence (middle), and to the combined effects of gravity wave drag and associated diffusion (bottom).

drag. Note the very small variability in temperature in the tropical and summertime regions which are dominated by radiative processes.

Equally as important as the ability of the model to produce reasonable year-to-year variability is the realism of the processes producing the changes. We have identified two processes, one which is widely recognized, and the other which has yet to be established. The first process is exemplified by the variation in the mean zonal wind between January of the second year and January of the third year (Fig. 5, top left). West winds were some 30 m s^{-1} less during the January of year 2, and, as indicated (Fig. 5, top right), this was due to changes which occurred during the month. The processes acting to decelerate the wind in this January relative to the following January are shown in the rest of the figure. The deceleration was apparently caused by greater EP flux convergences (Fig. 5, middle right), acting throughout the winter stratosphere, and overcoming the impact of the greater westerly acceleration due to transformed advection (Fig. 5, middle left). The change in gravity-wave drag played a minor direct role (Fig. 5, bottom). Similar correlations between monthly mean EP flux divergences and monthly mean zonal winds were found by Hamilton (1982) using the NOAA/NMC analysis for 1976–80, and Boville (1986) during perpetual January simulations with the NCAR CCM.

The greater EP flux convergence was associated with the greater eddy kinetic energy which existed between 20 and 70 km (Fig. 6, top). The changes in the vertical and northward EP fluxes (Fig. 6, bottom) indicate that the eddy energy was preferentially propagating upward from the troposphere in upper midlatitudes, and then southward to midlatitudes in the stratosphere. The eddy energy was actually less in the troposphere itself during this month; the greater upward propagation at the appropriate latitudes appears to be associated with the more favorable propagation conditions in the lower stratosphere, as approximated by the dominant term in the refractive index, $\delta q/\delta y/U$ (see Fig. 6, bottom, where the shaded regions indicate areas of significant negative changes). As evident in Fig. 5 (top left), the west winds were somewhat stronger in the lower stratosphere in January of year 2, affecting the ability of waves to propagate vertically, and the ability of eddies to decelerate the zonal wind. The importance of this process has been emphasized in numerous studies (e.g., Davies, 1981; Bridger and Stevens, 1982), and it occurs in a number of months in the model, in both hemispheres.

The second type of process which results in model variability is illustrated in Fig. 7 (top, left), which shows that the zonal mean winds were some 35 m s^{-1} less in February of year 3 than in February of year 4. Peak changes occur from 50° – 60°N . In much of this region the eddies were acting to provide a slightly smaller deceleration in year 3 (i.e., the change in EP flux diver-

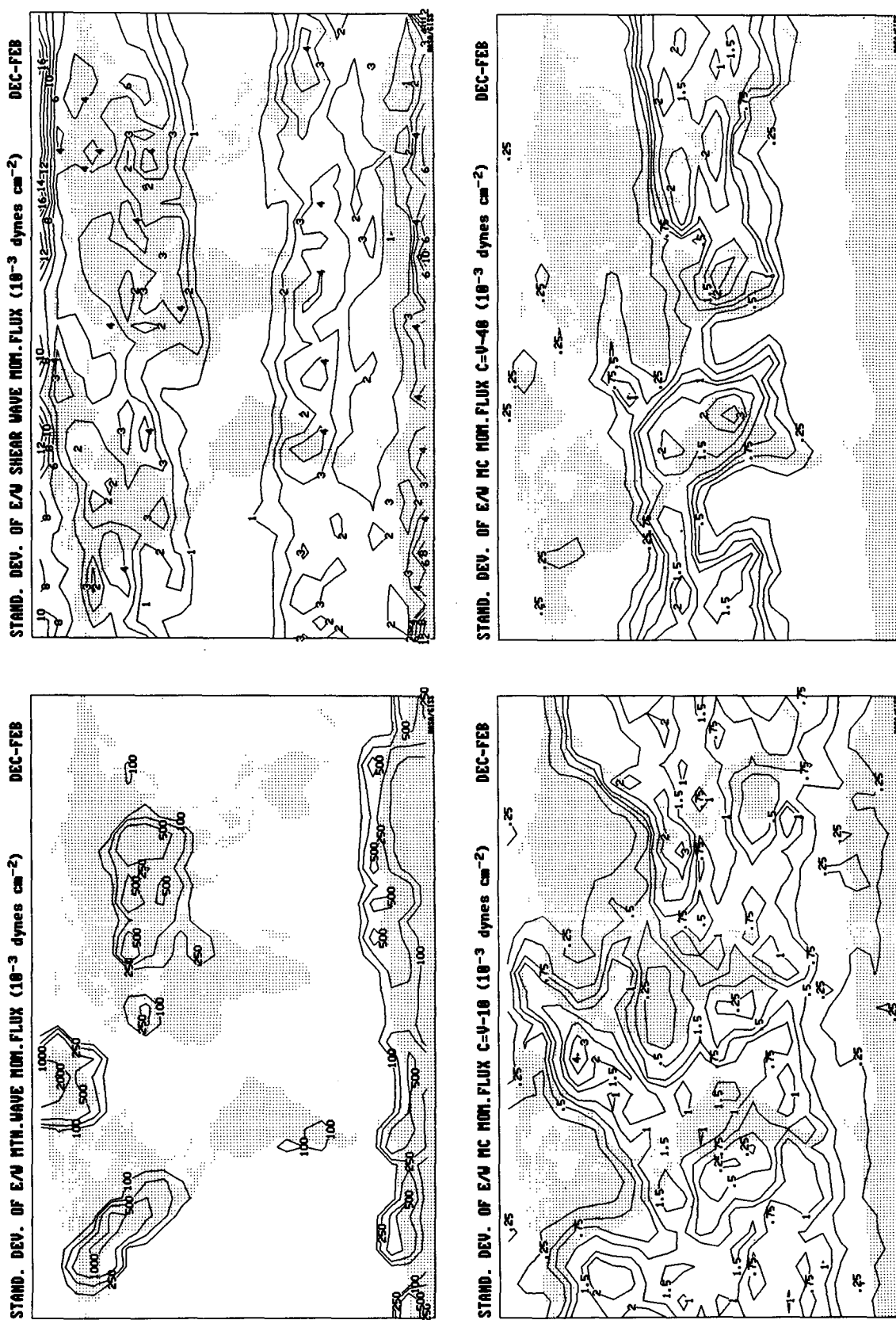


FIG. 3. Monthly average standard deviations averaged over the months of December-February of the parameterized gravity wave zonal momentum flux from topography (top left), from shear (top right), from moist convection with phase velocity $c = 10 - 40 \text{ m s}^{-1}$ (bottom left), and moist convection with phase velocity $c = 10 - 40 \text{ m s}^{-1}$ (bottom right). Momentum fluxes are calculated at lowest level of application, 583 mb for the topographic waves, and 100 mb for the other wave sources.

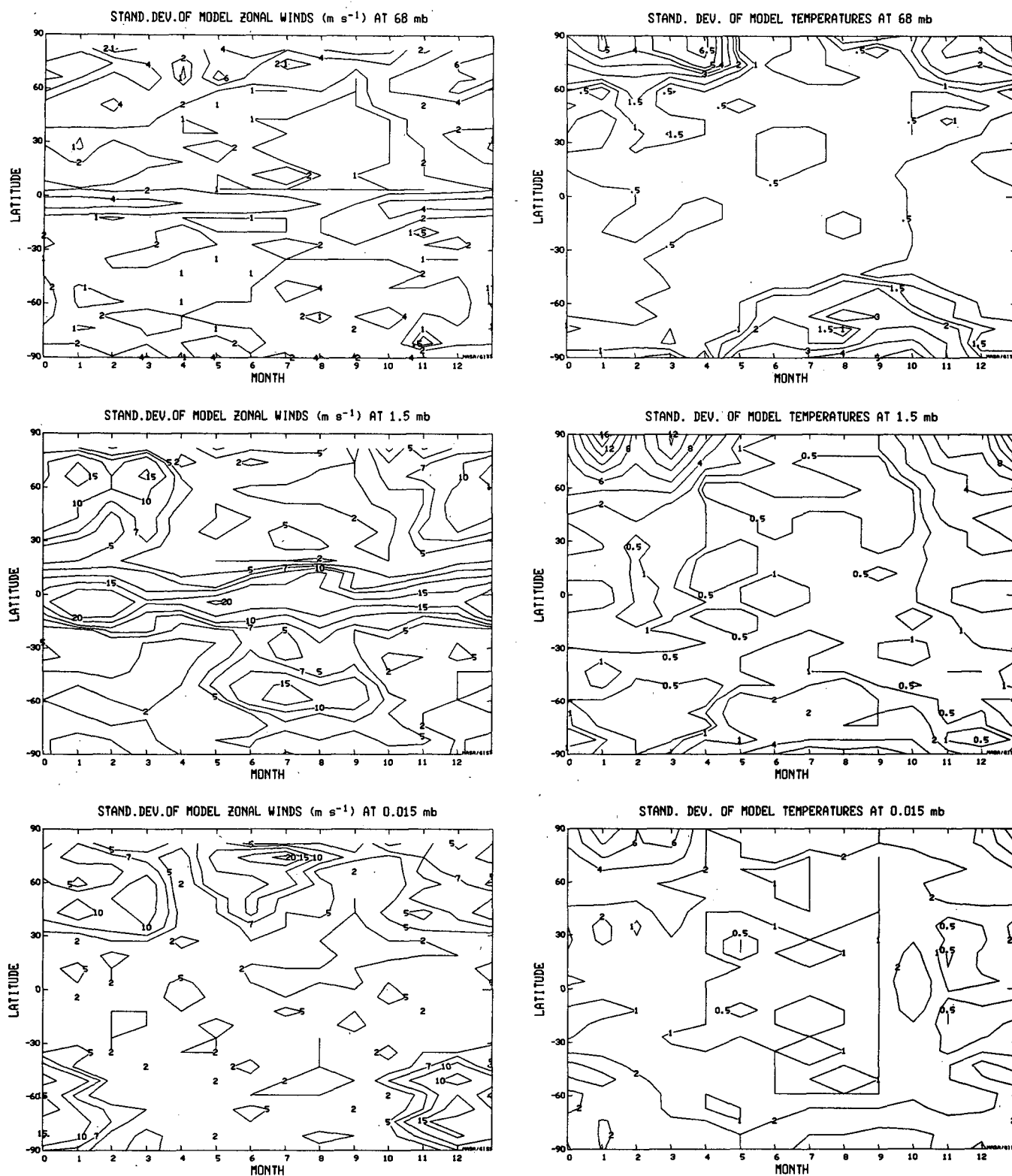


FIG. 4. Model standard deviation of the zonally averaged zonal wind (left) and temperature (right) for 68 mb (top), 1.5 mb (middle), and 0.015 mb (bottom). Note that both in this figure and in Figs. 1 and 2, the zonal averaging is taken before the standard deviation is calculated.

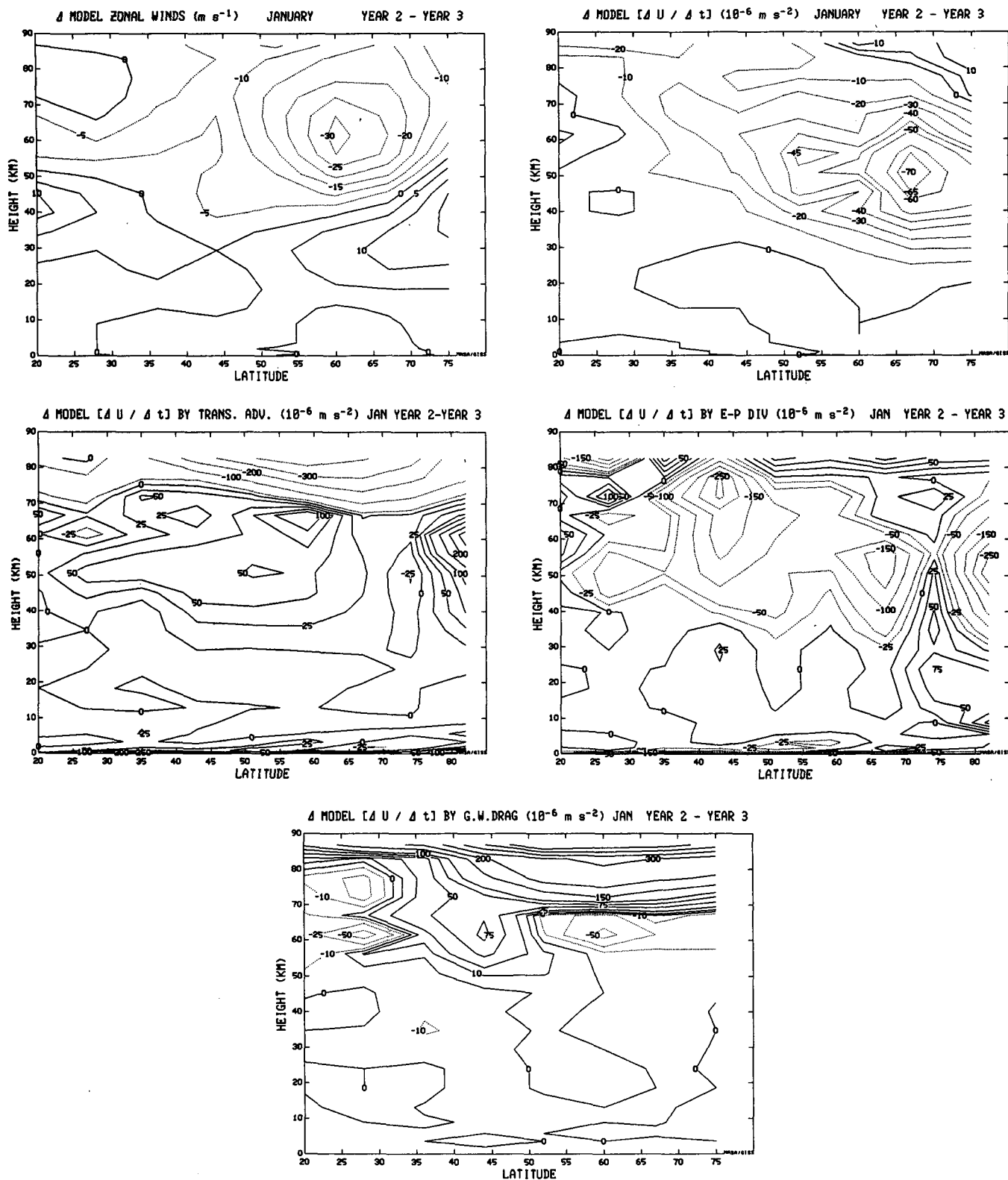


FIG. 5. The difference between model January of year 2 and year 3 in the zonal wind (top left), in the change of the zonal wind during the month (top right), in the change of the zonal wind by transformed advection (middle left), in the change of the zonal wind by EP flux divergence (middle right), and in the change of the zonal wind by parameterized gravity wave drag (bottom).

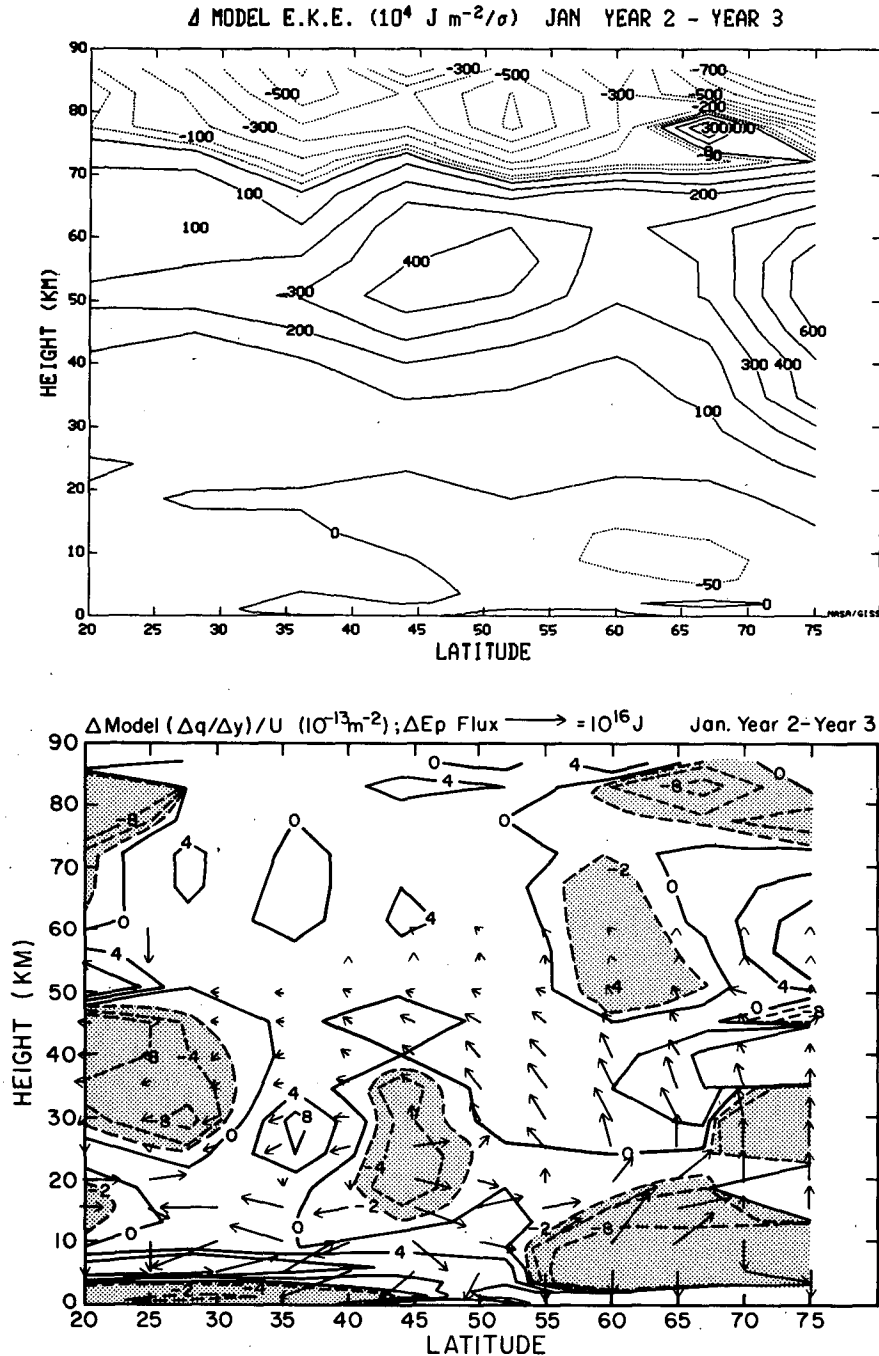


FIG. 6. The difference between model January of year 2 and year 3 in eddy kinetic energy (top), and the latitudinal gradient of the quasi-geostrophic potential vorticity normalized by the zonal wind (thus the leading term of the quasi-geostrophic refractive index), along with the change in the EP flux vectors (bottom). Significant negative changes in the refractive index term are shaded, and EP flux vector changes below 500 mb are limited in magnitude for presentation purposes.

gence was acting to provide a slightly greater acceleration of the westerlies in year 3, Fig. 7 bottom, right), and the eddy energy in February of year 3 was actually slightly less than that of year 4. The transformed advection was also producing greater acceleration (Fig.

7, top right). In this case, it is the change in gravity-wave drag associated with topography that is the major cause for the difference (Fig. 7, bottom left). As evident in the figure, the mountain wave drag is greater throughout the stratosphere; the difference between the

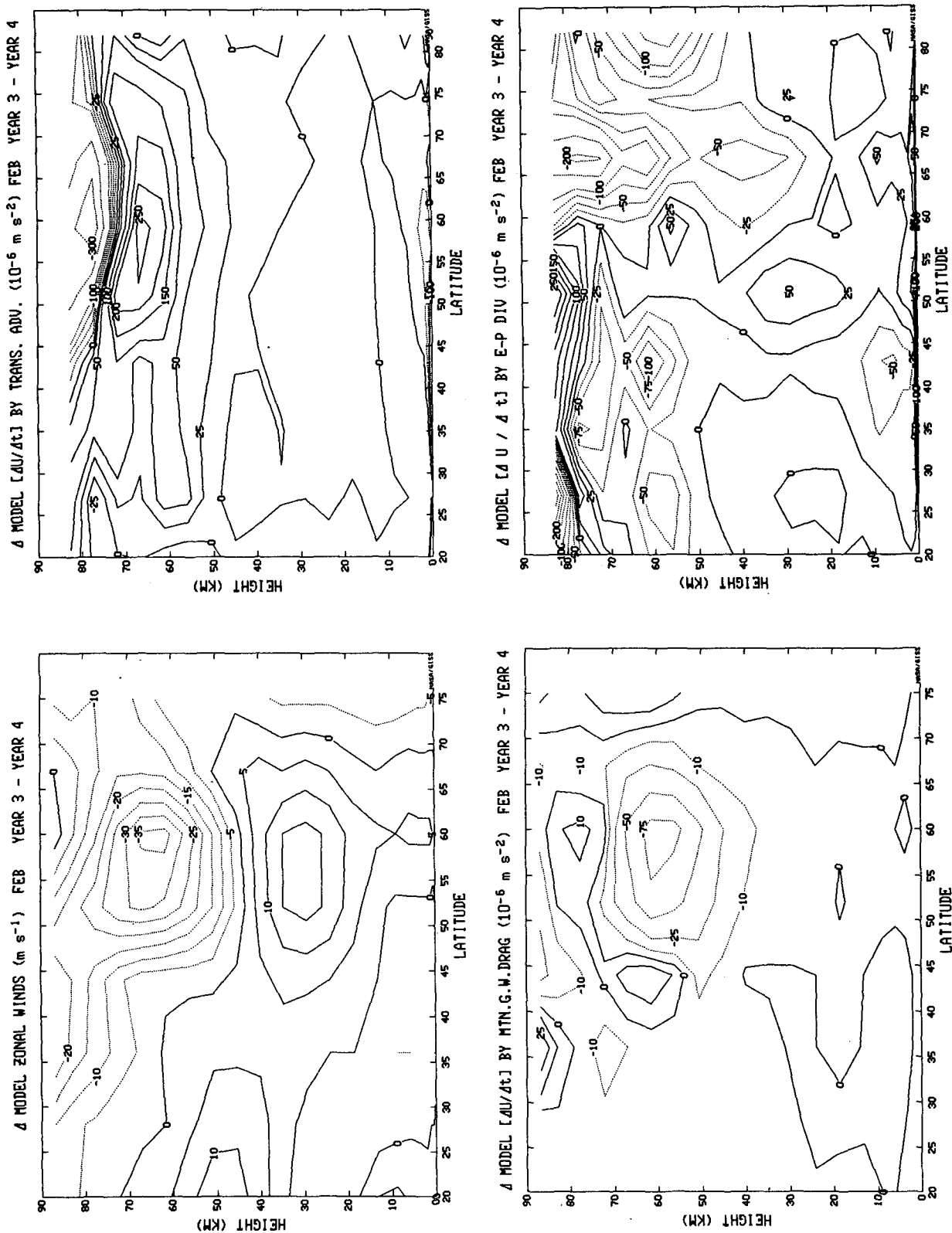


FIG. 7. The difference between model February of year 3 and year 4 in the zonal wind (top left), in the change of the zonal wind by transformed advection (top right), in the change of the zonal wind by parameterized gravity waves due to topography (bottom left), and in the change in the zonal wind by EP flux divergence (bottom right).

two months appears to be associated with stronger and more consistent west winds blowing over the regions of high topography during February of year 3. Variability induced by this process has not been reported, and may be difficult to detect. Note that even in the first process, the greater gravity-wave-induced drag (Fig. 5, bottom) would help the eddies decelerate the zonal mean flow by providing for a violation of the nonacceleration theorem conditions.

3. Model stratospheric warmings

During the five model years, midwinter warmings of various degrees occurred. The general pattern was for the warming to occur during the month of December, following a buildup of the zonal winds in November and early December. Observed warmings occur at any time between December and February (e.g., McInturff, 1978); however, while most observations of warmings were historically restricted to the middle stratosphere, we include in our definition lower mesospheric warmings as well, which are known to occur somewhat earlier (e.g., Entsian et al., 1971; Labitzke, 1981). As it is beyond the scope of this paper to describe these events in great detail, we will simply provide a brief overview of two of the warmings; the purpose is to emphasize the ability of the model to generate these important dynamical events realistically.

Shown in Fig. 8 are the temperature changes that occurred during December of year 1 (top left) and year 4 (top right). Strong temperature increases occurred during these months, maximizing at the North Pole. Accompanying these temperature rises are temperature decreases in the mesosphere and low-latitude stratosphere; this inverse correlation has been commonly observed (e.g., van Loon et al., 1975; Labitzke, 1981) and modeled (e.g., Matsuno, 1971), and is thought to result from changes in circulation and eddy forcing. The warming during December of year 1 was accompanied by large wave 1 amplitudes and small wave 2 amplitudes (Fig. 8, left middle and bottom), and is similar in this sense to the "wave 1" warming of 1977 (O'Neill and Taylor, 1979). The warming during December of year 4 had large wave 2 but small wave 1 amplitudes (Fig. 8, right, middle and bottom), and is thus similar to the "wave 2" warming of 1979 (Palmer, 1981a). This apposition of wave 1 and wave 2 amplitudes on the monthly average has also been observed (e.g., van Loon et al., 1975). Differences exist not only in the standing wave component of waves 1 and 2 but for the total wave energies as well; in both cases the total energy of the dominant wave was about four times that of the secondary wave in the region of 10–0.46 mb. Note also that the warming during year 4 occurred at a somewhat lower altitude than in year 1, as wave 2 amplitudes peak at a lower altitude.

The energy history of the warming during December of year 4 is presented in Fig. 9 (top), and that for December–January of year 1 in Fig. 9 (bottom). Zonal kinetic energy and zonal potential energy in the upper stratosphere decrease dramatically during the month, in apparent response to increases in eddy kinetic energy.

The energy history from the troposphere to the mesosphere for waves 1 and 2 for December of year 4 is shown in Fig. 10. This wave 2 warming is associated with an upward flux of eddy geopotential energy from lower levels; it is not a product of nonlinear interactions, and wave 2 is in fact losing energy to other wave numbers throughout the middle atmosphere. Note the varying wave 2 energy history in the troposphere, and the apparent upward propagation of eddy energy change, with a phase lag of about 6 days between the tropospheric and mesospheric peaks. This is in approximate agreement with the time lags observed by Muench (1965) during the January 1958 warming. The transient eddy energy forcing in the troposphere apparent in this figure is thought to be a likely cause of warmings (e.g., Davies, 1981). There is also evidence of "preconditioning", in that the major effect at the end of the month was preceded by a warming pulse some two weeks earlier, again an important phenomenon in the development of significant warmings (Palmer, 1981b). The first decrease in zonal kinetic energy during the middle of the month (Fig. 9, top) is associated with the erosion and diminution of the stratospheric vortex, which can be interpreted as making it more susceptible to subsequent wave activity (McIntyre and Palmer, 1984). Note also the apparent anticorrelation between wave 1 and wave 2 amplitudes in both the stratosphere and mesosphere, another often observed feature during warmings which appears to operate on short time scales as well as on the monthly average (Labitzke, 1977; Schoeberl, 1978).

The eddy available potential energy increases substantially in the upper stratosphere during the later, more significant warming (Fig. 9, top), and may contribute toward the generation of eddy kinetic energy at that time. Observational results of the importance of the baroclinic process seem to imply that such instability may exist during major warmings, especially those characterized as wave 2 warmings (McInturff, 1978).

The warming of December–January of year 1 was a wave 1 warming, (Fig. 8, left), and the events differ in some respects from the wave 2 warming of year 4. The increased eddy kinetic energy in the upper stratosphere is accompanied by less of an increase in eddy available potential energy (EAPE) (Fig. 9, bottom), and peak EAPE values barely exceed the background levels of earlier in the month. As noted in McInturff (1978), there is evidence that wave 1 warmings appear to have less direct baroclinic energy transfers than do the wave 2 events.

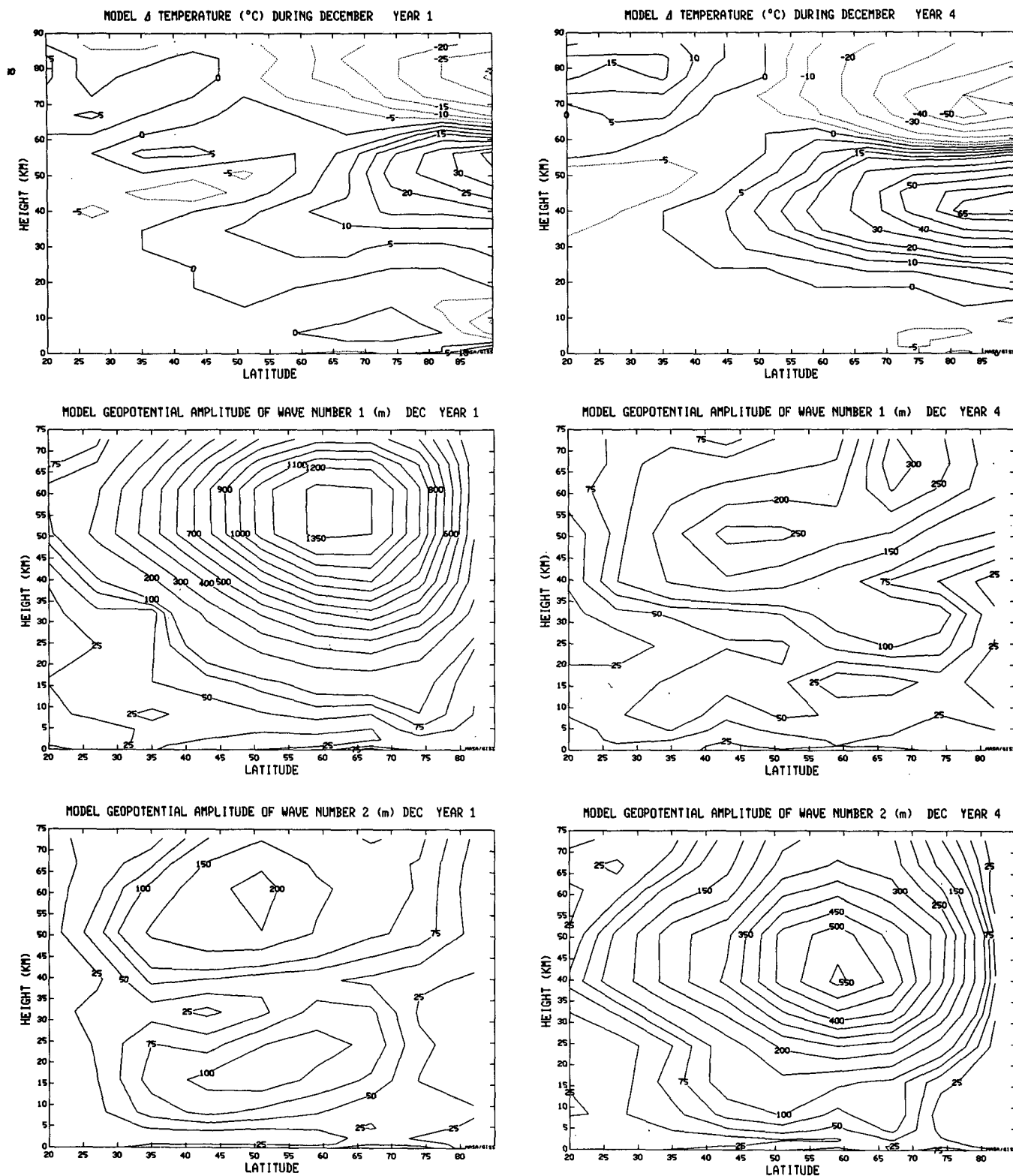


FIG. 8. Model temperature change during the month of December (top), geopotential amplitude of wavenumber 1 (middle), and geopotential amplitude of wavenumber 2 (bottom) for December of year 1 (left) and year 4 (right).

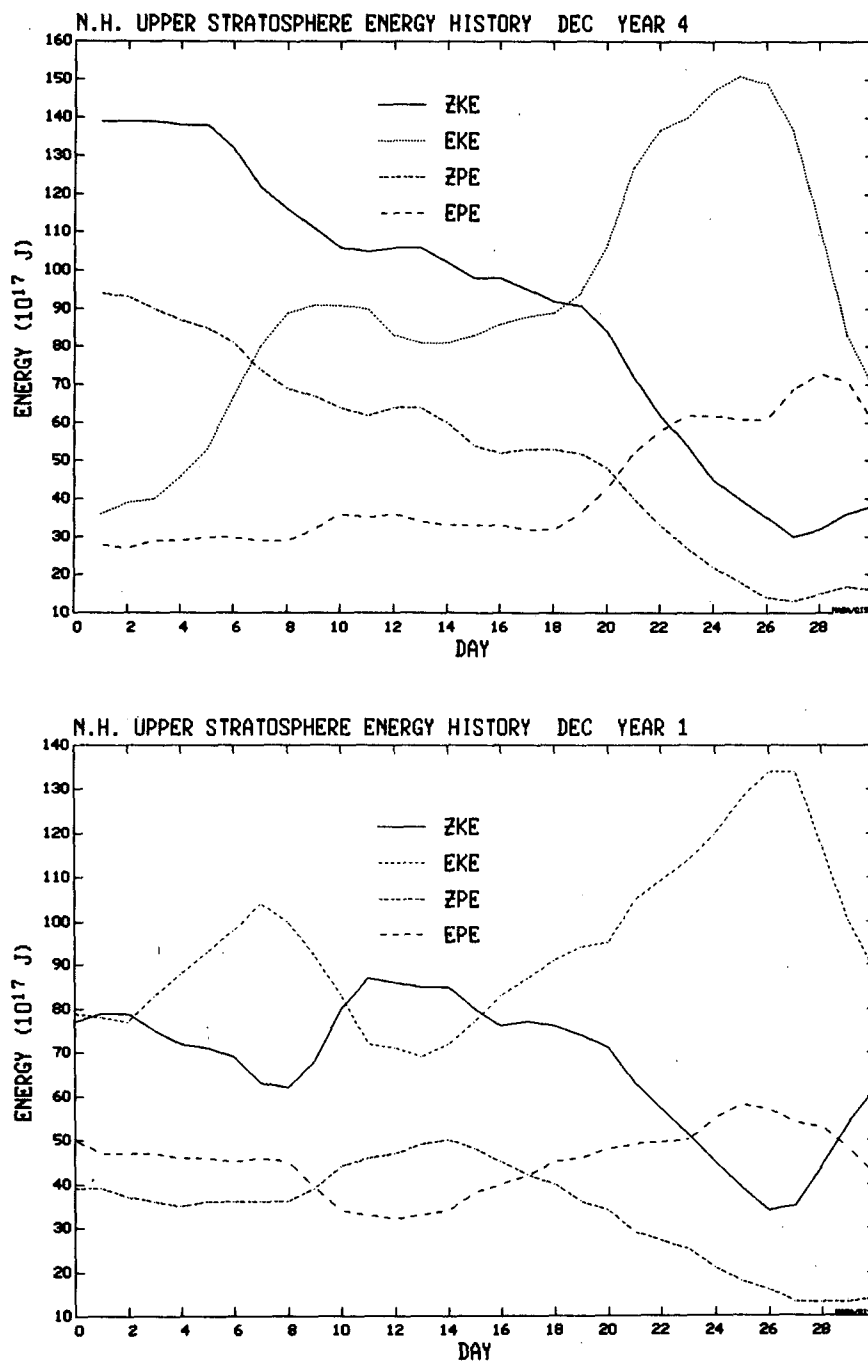


FIG. 9. Upper stratosphere (10 mb–0.46 mb) energy history during December of year 4 (top) and for 30 days beginning 10 December of year 1 (bottom) for zonal kinetic energy (ZKE), eddy kinetic energy (EKE), zonal available potential energy (ZPE), and eddy available potential energy (EPE).

The energy history of waves 1 and 2 for this warming is shown in Fig. 11. Again there is an apparent preconditioning, with a warming pulse several weeks earlier than the major event. There is again some indication of anticorrelation between wave 1 and wave 2

amplitudes, and there is a definite correlation between the peaks in tropospheric and middle atmosphere wave 1 energy values during the month. However, it is not at all obvious that the wave 1 energy peaks occur earlier at the lower levels, despite an upward eddy geopotential

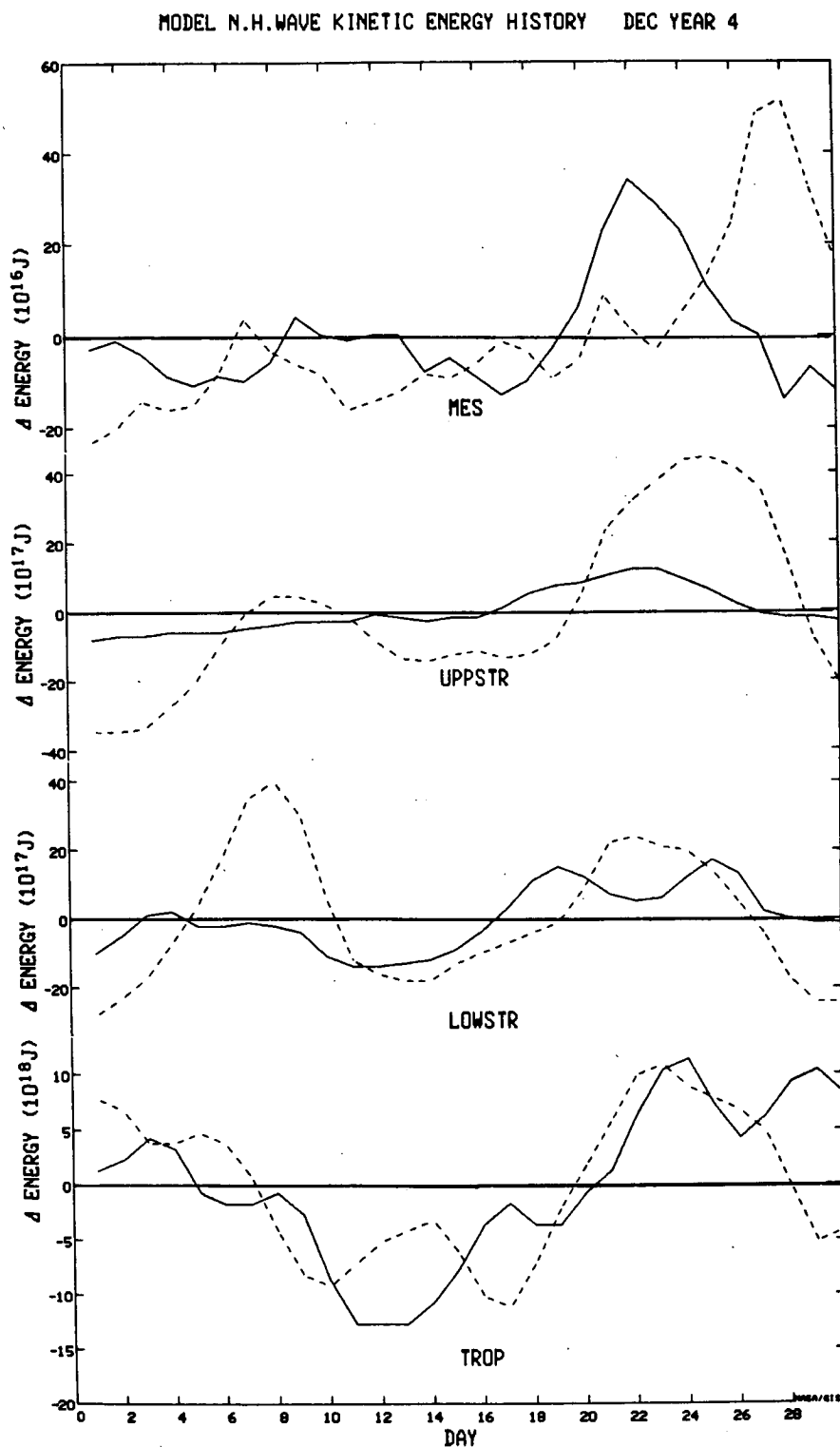


FIG. 10. Wave 1 (solid line) and wave 2 (dashed line) kinetic energy histories during December of year 4 for the troposphere (984–100 mb), lower stratosphere (100–10 mb), upper stratosphere (10–0.46 mb), and mesosphere (0.46–0.002 mb).

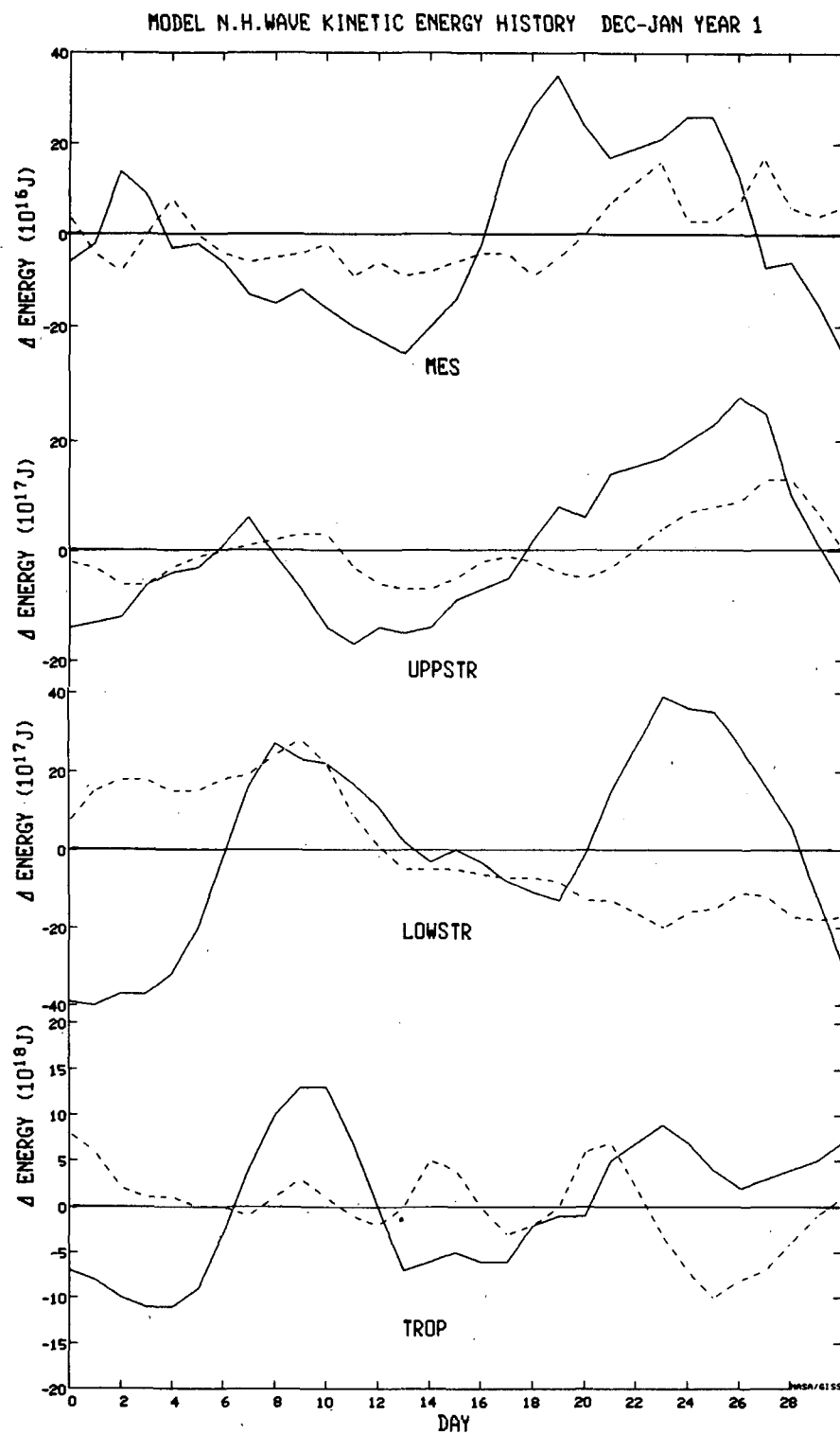


FIG. 11. As in Fig. 10, except for 30 days starting 10 December of year 1.

energy flux for the month as a whole. Only wave 1 in the troposphere is gaining energy due to nonlinear wave interactions.

4. Sensitivity of midwinter warmings to gravity wave drag

The preceding discussion related the development of the warming to the planetary wave forcing from the troposphere. Is there also an important contribution from the parameterized gravity wave drag? To investigate this, we can review the sensitivity experiments discussed in Part I, in which individual runs were made without the different gravity-wave drag sources. The experiments were conducted starting from 1 October, year 3, and run for three months. December of year 3 experienced a stratospheric warming in the control run, and it was of interest to determine how removal of the various gravity-wave drag mechanisms would affect this event. We focus on the response of the zonal wind field, as weakening of the wintertime jet accompanies high-latitude warmings.

As shown in Part I (Figs. 20, 21), all of the experiments produce substantially greater west winds in the winter stratospheric jet region in December. Different explanations apply in the different runs. The experiments with no mountain drag or no high phase velocity moist convective waves failed to produce the warming noted in the control run, even though the long-wave amplitudes were as high or higher. In the control run, EP flux convergences strongly decelerated the zonal wind. In these experiments, the lack of dissipation associated with gravity waves meant that the eddies were not as effective in acting on the zonal mean flow, and the warming did not develop. This is a clear example of how important dissipation in the model appears to be for the simulation of winter dynamic events and their irreversibility (as suggested by Rood, 1985). Note that in model 1, with no stratospheric momentum dissipation, wave amplitudes reached 2000 m before a warming developed.

In the runs with no shear moist convective drag, weak warmings occurred, but with no shear drag the high-latitude west winds were much stronger in November, and the difference was still evident in December. In both cases, the reduction in zonal winds which did take place occurred at somewhat lower latitudes. The change in dissipation also affects the entire development of the winter zonal wind profile, and the subsequent propagation conditions of both planetary waves and the parameterized gravity waves. In all of the cases, changes in the gravity wave forcing affected the character or even the very existence of the warming event.

5. Discussion

The model results emphasize the complexity of the relationships among the gravity wave dissipation, planetary wave energy and the mean zonal flow. The gravity wave dissipation brings about violations of the

nonacceleration conditions, enabling the eddies to alter the mean circulation. Changes in gravity wave dissipation result in changes in the way eddies affect the mean circulation, as well as changes in the direct dissipation of the eddies and mean circulation by the gravity waves. As the mean circulation changes, the ability of the gravity waves to propagate is altered, as well as the ability of the waves to break and decelerate the background flow. Changes in gravity wave breaking in the lower stratosphere can affect tropospheric energetics (see the discussion in Part I) which may impact the long-wave energy generation, and at the same time alter gravity wave generation processes. All this, in conjunction with the well-known dependence of the propagation conditions of eddies on the background flow structure, represents a complex set of interactions between the three processes, with multiple feedbacks of both a positive and negative nature.

While these results appear in the model, are there any indications that they occur in the real atmosphere? The ability of the model to produce reasonable interannual variations and stratospheric warmings implies that the model-generated variability is occurring in a realistic manner, but the comparison provides no guarantee of uniqueness. Direct verification depends on observations which are scarce, although Clark and Morone (1981) reported a specific example of mesospheric warming possibly associated with convectively generated gravity waves. Ground-based observations of gravity waves were made with a multipartite array of microbarovariographs at Lamont-Doherty Geological Observatory for over ten years (Balachandran and Donn, 1964). Tropospheric gravity waves were at their most consistently highest-amplitude during the times of stratospheric warmings, with large-amplitude waves recorded for a period on the order of one or two weeks during the time of developing stratospheric warmings. A particular example of this effect was discussed by Balachandran (1976) for the January 1974 stratospheric warming. To some extent, this consistency was a product of the blocking episodes which often precede such events, and the presence of high-amplitude gravity waves at the ground level does not necessarily imply that such waves were propagating into the stratosphere. Nevertheless, large-amplitude tropospheric gravity waves did occur preceding the warming. Were they to propagate vertically they would likely have had some effect, and due to their geographically consistent generation for the period of the blocking, they would have affected specific stratospheric locations in a more or less continuous fashion. What effect this would have had on the development of the warming, either directly or through their effect on planetary wave dissipation, has yet to be determined.

6. Conclusions

It is important for any model which is to be used for climate change assessments to have the proper sen-

sitivity. One method of investigating the model sensitivity is to determine how its variability on the interannual or intraseasonal time scales compares with that of the real atmosphere. In this respect, the model discussed here simulates variations of the right order of magnitude in the extratropics, and generates stratospheric warmings with many of the characteristics of the observed phenomenon. The variability may be excessive in the middle atmosphere tropics, in association with possible inertial oscillations, although observations now being made imply that the real world atmosphere may also be somewhat variable in this region.

The variability arises due to a complex interaction between gravity waves, eddies and the mean circulation. If this represents the real world situation, it poses a challenge for modelers of the impact of climate change on the middle atmosphere. It implies that changes in the gravity-wave generation, propagation, breaking and drag must be accurately assessed. This requires that the parameterizations and wave characteristics used in this and other models be verified through additional observations and theoretical developments. At present, the difficulty in modeling subgrid-scale phenomena such as convection is a major uncertainty in depicting the nature of future tropospheric climates, and subgrid-scale gravity-wave phenomena may provide additional uncertainty for the middle atmosphere.

Acknowledgments. Funding for this research was provided by the NASA Upper Atmospheric Research Program managed by D. Butler, and the ERBS/SAGE II Science Program through NASA Langley Research Center.

REFERENCES

- Arakawa, A., 1972: Design of the UCLA general circulation model. Tech. Rep. No. 7, Dept. Meteorology, University of California, Los Angeles, 116 pp.
- Balachandran, N. K., 1976: Atmospheric gravity waves: A case study, 2-4 January, 1974. *Bull. Amer. Meteor. Soc.*, **57**, 108 (abstract).
- , and W. L. Donn, 1964: Short and long period gravity waves over the northeast United States. *Mon. Wea. Rev.*, **92**, 423-426.
- Boville, B. A., 1986: Wave-mean flow interactions in a general circulation model of the troposphere and stratosphere. *J. Atmos. Sci.*, **43**, 1711-1725.
- Bridger, A. F. C., and D. E. Stevens, 1982: Numerical modeling of the stratospheric sudden warming: some sensitivity studies. *J. Atmos. Sci.*, **39**, 666-679.
- Clark, J. H. E., and L. T. Morone, 1981: Mesospheric heating due to convectively excited gravity waves—a case study. *Mon. Wea. Rev.*, **109**, 990-1001.
- Davies, H. C., 1981: An interpretation of sudden warmings in terms of potential vorticity. *J. Atmos. Sci.*, **38**, 427-445.
- Entsian, G., S. Gaygerov and D. Tarasenko, 1971: Midwinter warmings of the stratosphere and mesosphere and processes in the ionosphere. *Izv. Acad. Sci. U.S.S.R., Atmos. Oceanic Phys.*, **7**, 618-630.
- Finger, F. G., and S. Teweles, 1964: The midwinter 1963 stratospheric warming and circulation change. *J. Appl. Meteor.*, **3**, 1-15.
- Geller, M. A., M.-F. Wu and M. E. Gelman, 1984: Troposphere-stratosphere (Surface-55 km) monthly winter general circulation statistics for the Northern Hemisphere—Interannual variations. *J. Atmos. Sci.*, **41**, 1726-1744.
- Hamilton, K., 1982: Some features of the climatology of the Northern Hemisphere stratosphere revealed by NMC upper atmosphere analyses. *J. Atmos. Sci.*, **39**, 2737-2749.
- Hansen, J., G. Russell, D. Rind, P. Stone, A. Lacis, S. Lebedeff, R. Ruedy and L. Travis, 1983: Efficient three-dimensional global models for climate studies: models I and II. *Mon. Wea. Rev.*, **111**, 609-662.
- Hitchman, M. H., and C. B. Leovy, 1986: Evolution of the mean state in the equatorial middle atmosphere during October 1978–May 1979. *J. Atmos. Sci.*, **43**, 3159-3176.
- Labitzke, K., 1977: Interannual variability of the winter stratosphere in the Northern Hemisphere. *Mon. Wea. Rev.*, **105**, 762-770.
- Matsuno, T., 1971: A dynamical model of the stratospheric sudden warming. *J. Atmos. Sci.*, **28**, 1479-1494.
- McInturff, R. M., 1978: Stratospheric warmings: synoptic, dynamic and general-circulation aspects. NASA Ref. Pub. 1017, 166 pp.
- McIntyre, M. E., and T. N. Palmer, 1984: The surf zone in the stratosphere. *J. Atmos. Terr. Phys.*, **46**, 825-849.
- Muench, H., 1965: On the dynamics of the winter stratospheric circulation. *J. Atmos. Sci.*, **22**, 349-360.
- O'Neill, A., and B. F. Taylor, 1979: A study of the major stratospheric warming of 1976/77. *Quart. J. Roy. Meteor. Soc.*, **105**, 71-92.
- Oort, A., 1977: The interannual variability of atmospheric circulation statistics. NOAA Prof. Pap. 8, 76 pp.
- Palmer, T. N., 1981a: Diagnostic study of a wavenumber 2 stratospheric sudden warming in a transformed Eulerian-mean formalism. *J. Atmos. Sci.*, **38**, 844-855.
- , 1981b: Aspects of stratospheric sudden warmings studied from a transformed Eulerian-mean viewpoint. *J. Geophys. Res.*, **86**, 9679-9687.
- Quiroz, R. S., 1981: The tropospheric-stratospheric mean zonal flow in winter. *J. Geophys. Res.*, **86**, 7378-7384.
- Rind, D., R. Suozzo and N. K. Balachandran, 1988: The GISS Global climate/middle atmosphere model. Part I: Model structure and climatology. *J. Atmos. Sci.*, **45**, 329-370.
- Rood, R. B., 1985: A critical analysis of the concept of planetary wave breaking. *Pure Appl. Geophys.*, **123**, 733-755.
- Schlesinger, M. E., and J. F. B. Mitchell, 1987: Model projections of the equilibrium climatic response to increased CO₂. *Rev. Geophys.* (in press).
- Schoeberl, 1978: Stratospheric warmings: observations and theory. *Rev. Geophys. and Space Phys.*, **16**, 521-538.
- van Loon, H., R. A. Madden and R. L. Jenne, 1975: Oscillations in the winter stratosphere. *Mon. Wea. Rev.*, **103**, 154-162.